Journal of Colloid and Interface Science 350 (2010) 523–529

Contents lists available at ScienceDirect

Journal of Colloid and Interface Science

www.elsevier.com/locate/jcis

Aggregation of wedge-shaped perylenetetracarboxylic diimides with a different number of hydrophobic long alkyl chains

Lin Xue [a], Yanfeng Wang [a], Yanli Chen [b], Xiyou Li [a,*]

[a] Key Lab of Colloid and Interface Chemistry, Ministry of Education, Department of Chemistry, Shandong University, Jinan 250100, China
[b] Department of Chemistry, University of Jinan, Jinan 250001, China

ARTICLE INFO

Article history:
Received 19 May 2010
Accepted 9 July 2010
Available online 13 July 2010

Keywords:
Perylenetetracarboxylic diimides
Long alkyl chains
Aggregation
Nano-rod

ABSTRACT

Three perylenetetracarboxylic diimide (PDI) derivatives comprising a different number of hydrophobic alkoxy chains at one imide nitrogen were synthesized. The aggregation behavior of this series of compounds was investigated by UV–vis absorption and emission spectra. The results indicated that large number of hydrophobic alkyl chains at one end of the PDI molecules can induce significant aggregation in solution, but without obvious ground state interaction between the PDI aromatic cores. The aggregation behavior of this series of compounds in solid state was studied by absorption and IR spectra as well as X-ray diffraction (XRD) experiments. The morphology of the solid aggregates was investigated by scanning electronic microscopy (SEM). With an increase of the number of alkyl chains at one end of these PDI molecules, the aggregation mode varies from *H* type to *J* type, while the morphology of the solid aggregates changes from small bending belts to long ordered wires. This research demonstrated that one can control the aggregation mode, the order, and the morphology of the molecular aggregates by changing the number of alkyl chains. This information can be useful in the design of novel organic materials which exhibit molecular aggregation.

1. Introduction

Perylenetetracarboxylate diimides (PDI) are currently being investigated for use as a variety of photoactive organic materials because of their low light and thermal fading rates, high luminescence efficiency, and unique optoelectronic properties [1–4]. They were used in organic field-effect transistors, light-harvesting solar cells, and light emitting diodes as robust organic dyes [5–13]. They were proved to be excellent building blocks for self-organized molecular materials with highly ordered structure due to the strong π–π interactions between the planar PDI rings [14–21].

Introducing hydrophobic interactions between PDI derivatives by connecting long flexible hydrophobic alkyl chains to PDI molecule is a very efficient way to construct ordered molecular self-assembly. Würthner and co-workers had successfully connected tridodecylphenyl or tridodecyloxylphenyl groups to the imide nitrogen positions of PDI ring, which brought liquid crystal properties to PDI molecules [22,23]. Wasielewski and co-workers reported the self-assemble of tridodecyloxylphenyl substituted PDIs with pyrrolidinyl groups at the bay positions [24]. Very recently, Zang and co-workers reported the self-assemble of PDIs with long alkyl chains at the imide nitrogen position but no substituent at the bay substitutions [25]. Würthner reported recently that the morphology of the aggregates of PDI molecules was also controlled by the molecular shape [19]. A wedge-shaped amphiphilic PDI molecule preferred to form a vesicle like molecular aggregates while a dumbbell-shaped PDI was more likely to form rod-like molecular aggregates. All the work mentioned above, revealed that the combination of long alkyl side chains together with the strong π–π interactions between PDI aromatic cores could tune the self-assembly process. In order to achieve a highly ordered structure by controllable self-assemble process, the key factor is to reach an optimum balance of π–π interactions and hydrophobic interaction between alkyl chains.

Up to now, the PDI compounds substituted with trialkyloxylphenyl group are mostly symmetrically connected at the imide nitrogen atoms or the bay positions, unsymmetrically substituted PDIs with trialkyloxylphenyl groups connected at only one end of PDI molecules are scarcely reported in the literature. We present here the synthesis and aggregation behavior of a series of novel wedge-shaped PDIs with trialkyloxylphenyl groups connected to the one end of the PDI core. Because of the different size of the hydrophobic side chains, the self-assemble properties of these compounds vary dramatically. The finding of this research will be helpful on the design of new PDI based functional materials with controllable photophysical properties, micro-structure and morphology.

---

* Corresponding author. Fax: +86 531 88564464.
E-mail address: xiyouli@sdu.edu.cn (X. Li).

0021-9797/$ - see front matter © 2010 Elsevier Inc. All rights reserved.
doi:10.1016/j.jcis.2010.07.012

2. Materials and methods

2.1. General methods

Electronic absorption spectra were recorded on a Hitachi 4100 spectrometer. Fluorescence spectra were measured on an ISS K2 system. The fluorescence quantum yields were calculated with monomer as a standard. The low-angle X-ray diffraction (LAXD) experiment was carried out on a Rigaku D/max-γ B X-ray diffractometer. SEM images were obtained using a JEOL JSM-6700F field-emission scanning electron microscopy. For SEM imaging, Au (1–2 nm) was sputtered onto the grids to prevent charging effects and to improve image clarity. The minimized structure of the molecules were calculated by the B3LYP method and 6-31G (d) basis set in Gaussian 03 program.

3. Results and discussion

3.1. Synthesis

An overview of the structure of the title compounds (**1**–**3**) and the synthetic procedures are shown in Scheme 1. The 1,7-disubstituted PDI was chosen as the PDI core because it had not only strong π–π interactions but also good solubility in conventional organic solvents. The good solubility in organic solvents can simplify the synthetic and purification procedures significantly.

N-cyclohexyl-1,7-di(p-*t*-butyl-phenoxyl)-3,4-dicarboxylic imide-9,10-dicarboxylic anhydride (**4**) reacts with hydrazine in $CHCl_3$ to give N-amine-N′-cyclohexyl-1,7-di(p-*t*-butyl-phenoxyl)-3,4,9,10-tetracarboxylic diimide (**5**), which further reacts with 1,3,5-trichloride-2,4,6-triazine to give the important intermediate **6**. Compound **6** reacts with 3,4,5-trialkoxylaniline [26] to give the wedge-shaped compound **1**. Compounds **2** and **3** were prepared by the reaction of **4** with **7** or 3,4,5-trialkoxylaniline in toluene/imidazole. All the new compounds were fully characterized with ^{1}H NMR, MALDI-TOF mass spectra, as well as elemental analysis.

3.2. UV–vis absorption spectroscopy

UV–vis absorption spectra are sensitive to interchromophore distance and orientation [27] and therefore have been used widely to study the self-assemble process of chromophores with large π system [28–30].

Fig. 1 shows the absorption spectra of these three compounds (**1**–**3**) in toluene at different concentrations. All these compounds present maximum absorption band around 540 nm (0–0 transition), which is accompanied with a small shoulder at about 508 nm (0–1 transition) [31]. The absorption spectra of compound **1** do not change along with the concentration increase, which suggests that there is no significant ground state interaction between the PDI core of compound **1** even in a concentrated solution (the largest concentration tested in the experiments is 1×10^{-3} mol L^{-1}). But the situation changes when the number of alkyl chains decrease as revealed by the absorption spectra of compounds **2** and **3**. With the increase on the concentration of compound **2** in toluene, the intensity of the absorption band around 540 nm decreases obviously while that of the small shoulder at 510 nm increases slightly. Small red-shifts are observed for the both two absorption bands at 540 (inset of Fig. 1B) and 506 nm. The band centered at 540 nm red-shift for about 4 nm to 544 nm when the concentration of **2** in toluene increased from 1×10^{-5} to 1×10^{-3} mol L^{-1}. Almost equal red-shift is observed for the small

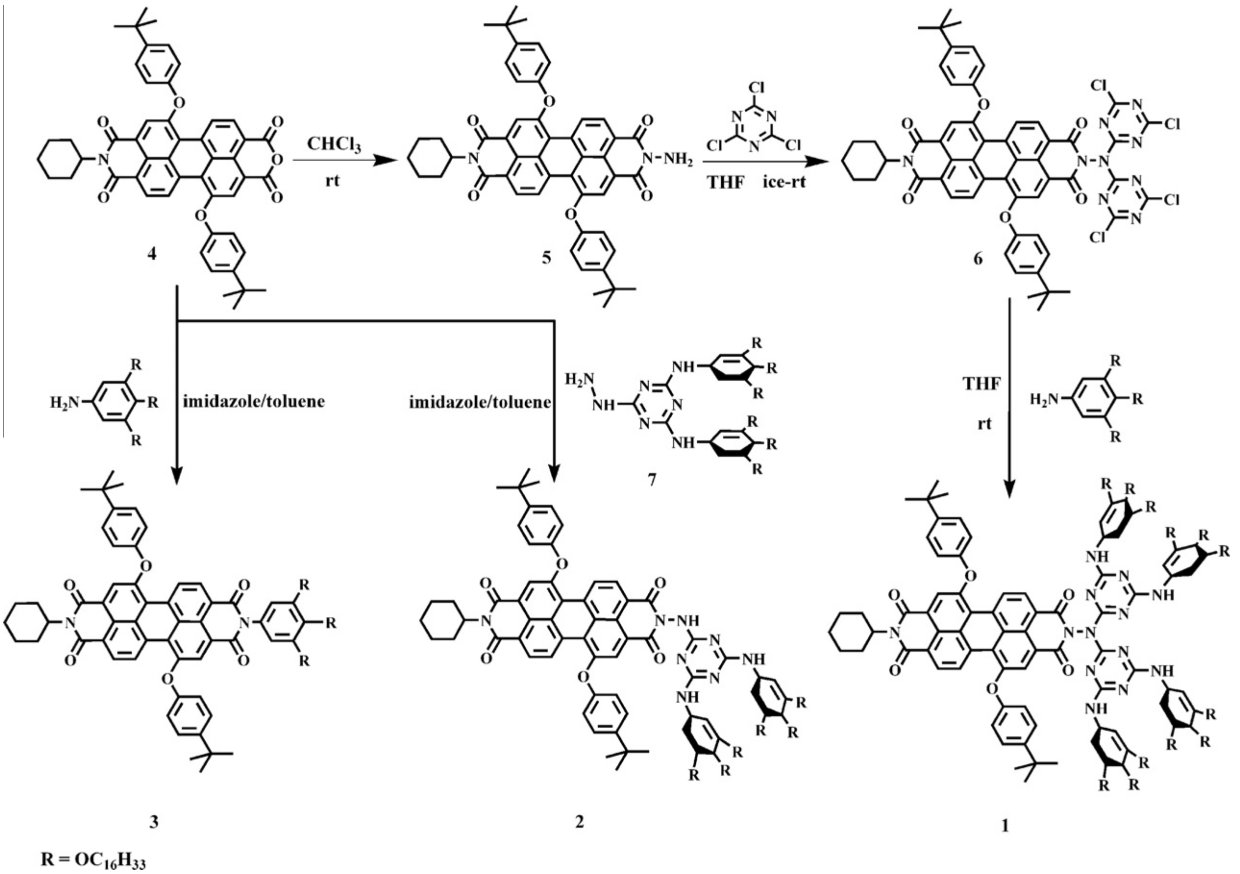

Scheme 1. Synthesis of **1**–**3**.

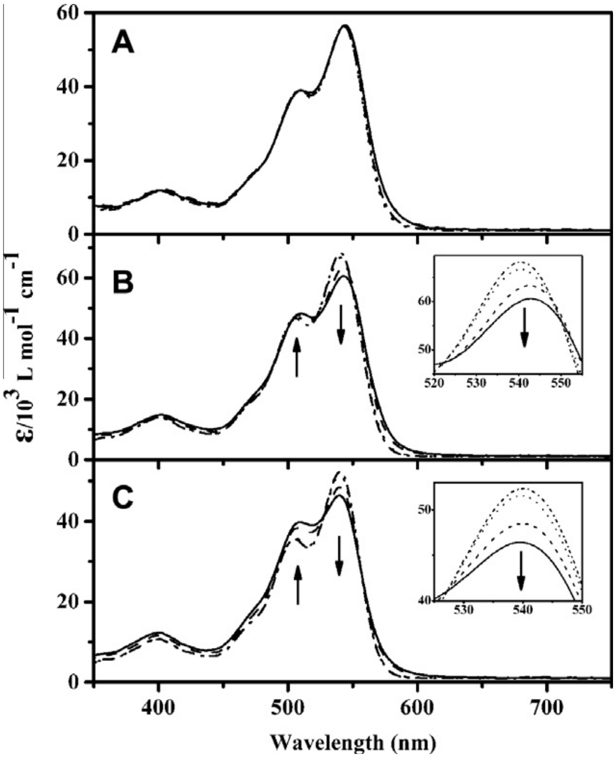

Fig. 1. Concentration-dependent UV–vis absorption spectra of compounds **1**–**3** in toluene. (A) Compound **1**, (B) compound **2**, (C) compound **3**. Concentrations are 1×10^{-5} M, 5×10^{-5} M, 5×10^{-4} M, and 1×10^{-3} M respectively. Arrows indicate the direction of concentration increase. Inset of Fig. 1B and C shows the magnified maximum absorption band of the two compounds.

band centered at 508 nm. Intensity decrease for the band at 540 nm and intensity increase for the band at 506 nm are observed for compound **3** along with the concentration increase, but without obvious band shift is observed for the maximum absorption band at 540 nm. This observation suggests that the ground state interaction between the molecules of **2** or **3** increase significantly along with the concentration increase. The ground state interactions between the molecules of **2** or **3** may be caused by molecular aggregation at high concentrations.

According to the previous report, the 0–0 and 0–1 transition will reverse in intensity upon π–π stacking [32], therefore, the intensity changes on the absorption bands observed for compounds **2** and **3** at high concentration maybe caused by the formation of face-to-face stacked molecular aggregates. Normally, an exactly face-to-face stacked dimer of PDI will give an absorption spectrum with the intensity of 0–0 transition smaller than that of 0–1 transition [33]. This completely intensity reverse is not observed in the absorption spectra of compounds **2** and **3** at higher concentrations, which suggests either a slipped face-to-face stacked structure for the molecular self-assembly or the existence of large portion of non-aggregated PDI molecules in the solution because of the low stability of the molecular self-assembly. Following exciton theory, shift on the absorption band of planar chromophore on aggregation is determined by the angle between the line connecting the centers of the two neighboring molecules and the normal of the molecular plan. If the angle smaller than 54.7° (the magic angle), the absorption band will blue-shift and the aggregates formed is defined as *H* aggregates. When the angle is larger than 54.7°, the absorption band will move to red and the aggregates is defined as *J* aggregates [34]. The small red-shift observed for the absorption bands of compound **2** at high concentrations are therefore can be attributed to the formation of *J* aggregates. However, the red-shift observed for the aggregates of compound **2** is smaller than that observed for the aggregates of other PDIs in the literature [35]. This may be attributed to the large center-to-center distance between neighboring molecules in the aggregates of compound **2**, which reduce the interactions significantly and thus lead to the small red-shift. No band shift was observed for the absorption band for compound **3** at high concentrations, which suggest the formation of *H* aggregates.

3.3. Fluorescence spectra

The fluorescence spectra of PDIs are also sensitive to the aggregation, therefore, it was employed previously in the study of self-assembly of PDI too [1]. The fluorescence spectra of compounds **1**–**3** show similarly one broad band centered at about 580 nm. The shape and wavelength of this emission do not change along with concentration increase, but the fluorescence quantum yields decrease significantly. Previous research had revealed that the formation of both *H* and *J* aggregates induce new broad emission band at long wavelength. The missing of new emission band at long wavelength in the aggregates of compounds **1**–**3** in the fluorescence spectra does not rule against the formation of *H* or *J* aggregates for compounds **2** and **3** in concentrated solution, because the presence of photoinduced intramolecular electron transfer from the triazine part to PDI unit in compounds **1**–**3** has reduce the fluorescence quantum yields of them significantly [9]. We use the fluorescence quantum yields of the most diluted solution tested in our experiments as standard (Φ_0), by comparing the fluorescence quantum yields at more concentrated solutions (Φ) with Φ_0 (Φ/Φ_0), we got the quantitate effects of the concentration on the fluorescence quantum yields. Fig. 2 shows the plots of Φ/Φ_0 against the concentrations for compounds **1**–**3**. It can be found that the fluorescence quantum yields drop significantly along with the concentration increase. This fluorescence quantum yield drop can be ascribed to the so called “self-absorption phenomenon”, i.e. the emission from one molecule is absorbed by the neighboring molecules due to the very close arrangement of these two molecules. From the plot shown in Fig. 2 we can find that the fluorescence quantum yields of compounds **1**–**2** start to drop sharply at very low concentrations while a higher concentration is need for compound **3** and model compound **8** (N,N′-dicyclohexyl-1,7-di(p-*t*-butyl-phenoxyl)-3,4,9,10-tetracarboxylic diimide, the structure is shown in supplementary materials) to show large fluorescence quantum yield drop. The drop on the fluorescence quantum yields

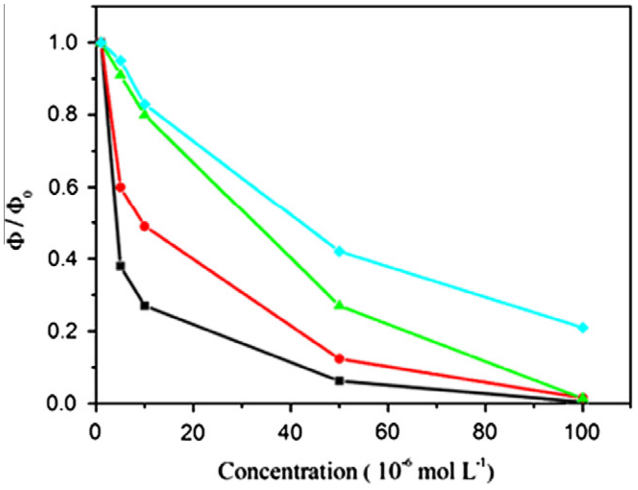

Fig. 2. The plots of Φ/Φ_0 against the concentrations for compounds **1**–**3** (■, **1**; ●, **2**; ▲, **3**) and model compound **8** (♦).

for compounds **1**–**2** can be ascribed to the formation of molecular self-assembly, which causes local concentration increase and thus induce the happening of "self-absorption". This result suggests that the long hydrophobic alkyl chains in compounds **1**–**2** have indeed induced significant molecular self-assemble at low concentrations and thus caused obvious fluorescence quenching. Φ of compound **1** drop sharply at very low concentrations as shown in Fig. 2. It reduced to one to third when its concentration increased from 1×10^{-6} to 1×10^{-5} mol L^{-1}. But the same magnitude of concentration increase induced only 50% decrease on Φ of compound **2** and 30% decrease on the Φ of compound **3**. This difference between compounds **1**–**3** suggests that the introduction of more alkyl chains in these molecules will increase the self-assemble ability in diluted solution.

The absorption spectra revealed that the concentration increase of compound **1** did not induce significant changes on the absorption spectra. The results deduced from the fluorescence measurement as mentioned above seems controversial to the results of the absorption spectra at first glance, but this is not true. The unchanged absorption spectra of compound **1** along with the concentration increase suggests only that no ground state interactions between the PDI units of different molecules, it is not the evidence of non-aggregation of the entire molecule. But contrarily, compound **1** self-assembled into molecular aggregates at very low concentrations driven by the strong hydrophobic interactions between the alkyl chains. Because of the large volume of the long alkyl chains, the PDI units can only pileup with large space between the neighboring PDI units and hereby no ground state interaction between PDI units is observed. In compounds **2** and **3**, both the volume of the long alkyl chains and hydrophobic interactions between the alkyl chains are relatively smaller than that in compound **1**, the π–π interaction between the PDI units is strong enough to interfere with the self-assemble process. Therefore, the PDI units can take a more closely packed conformation and ground states interactions between the PDI unites can be detected by the absorption spectra.

3.4. Aggregation in solid states

In order to investigate the effects of the long alkyl chains on the aggregation behavior of these wedge-shaped molecules in solid states, the thin solid films of these compounds are prepared by simply spreading drops of toluene solution of these compounds onto the surface of substrate. After evaporation of the solvents, the thin solid films are characterized by different physical methods.

The UV–vis absorption spectra of these thin solid films of compounds **1**–**3** are compared in Fig. 3. Comparing with that of monomeric PDI (compound **8**) in solution, obvious band broadening is observed in all these series of compounds due to the effect of the closely compacted molecular assembly [36,37]. For compound **1** with the most alkyl chains at one end of PDI in all these series of compounds, a large red-shift of the maximum absorption band is observed comparing with that of monomeric PDI, indicating that the formation of *J* aggregates in solid states [38]. Contrarily, for compound **3** with the least alkyl chains, the prominent feature of the absorption spectra is a reduction on the ratio of 0–0/0–1 transition intensity, along with significant blue-shift of the absorption maximum, and a loss of the fine structure. These features suggest the formation of face-to-face stacked *H* aggregates in solid states [39,40]. Dramatic change in absorption spectrum has also been displayed by the thin solid film of compound **2**. The relatively higher absorption at shorter wavelength implies the enhancement of the 0–1 transition due to the π–π interaction within the molecular aggregate. Comparing to the absorption of individual molecules of compound **8**, the absorption of compound **2** in solid state shifts slightly to red, which implies weaker (distorted) π–π interactions in the aggregate of compound **2** than that of compound **3** but stronger than that of compound **1** [41].

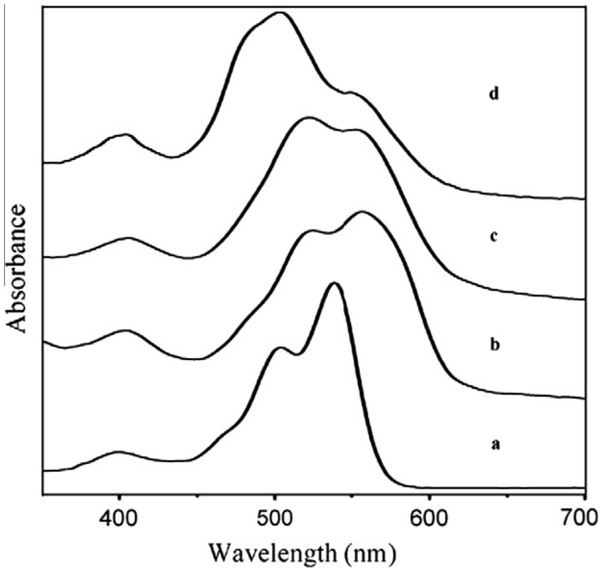

Fig. 3. Electronic absorption spectra of the thin solid films of compound **1** (b), compound **2** (c) and compound **3** (d) prepared from evaporation of drops of their toluene solution on a quartz plate as well as model compound **8** (a, 1×10^{-5} M) in toluene.

Since the electronic properties of compound **1**–**3** are essentially the same when dispersed as free molecules (see Fig. 1), the strikingly different absorption spectra observed for the aggregate states of the three molecules are most likely due to the different molecular packing conformation in the molecular assembly caused by the different number of alkyl chains [42,43]. As seen below, such a different molecular packing conformation results in a different dimensional preference for the growth of the molecular assembly.

3.5. IR spectra

In order to reveal the conformation and packing behavior of the long alkyl chains in the aggregates of compound **1**–**3**, IR spectra of the thin solid films of compounds **1**–**3** are recorded. The widths, relative intensities as well as the frequencies of the methylene stretching bands provide the information of orientation and order of the long alkyl chains in the molecular assembly [44,45]. The samples for the IR measurement are deposited onto a KBr disk from a concentrated toluene suspension. A uniform film is obtained after toluene evaporation. The measured IR spectra of the three compounds are shown in Fig. 4. Two sharp and intense peaks are observed at 2924 and 2853 cm^{-1}, which are assigned to the ν_a and ν_s CH_2 stretching bands, respectively [46,47]. The small shoulder at about 2960 cm^{-1} can be assigned to the vibration of CH_3 stretching. The frequencies, intensities, and bandwidths of the ν_a and ν_s CH_2 stretching bands match those of very highly ordered *n*-alkanethiol SAMs [48], therefore, it can conclude that the alkyl chains of these three compounds in their thin solid films packed with high order. The larger intensity of the stretching bands of compounds **1** and **2** relative to that of compound **3** indicates that the long alkyl chains of compounds **1** and **2** pack with higher order than that of compound **3** [49,50].

3.6. X-ray diffraction patterns

The molecular orders in the solid state are also investigated by the X-ray diffraction experiments. For all the compounds, the X-ray

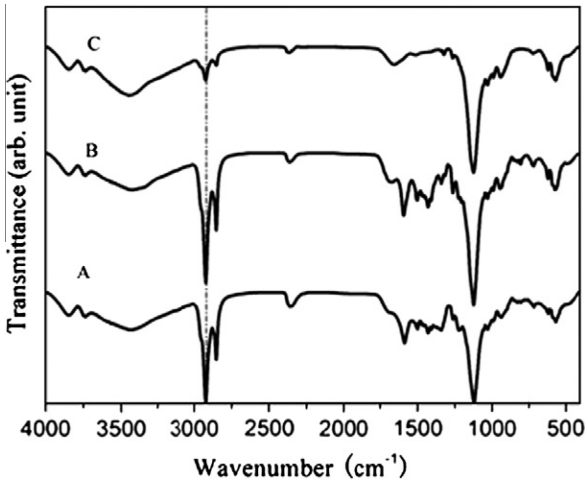

Fig. 4. IR spectra of the thin solid films of compounds **1**–**3** (A–C) prepared from evaporation of drops of their toluene solution.

diffraction patterns are characterized by a broad peak at $2\theta = 21°$ corresponding to the d value of 0.42 nm that relate to the liquid-like order of the alkyl chains [22], which is well consistent with the results of IR spectra. As shown in Fig. 5, the thin solid film of compound **1** presents the strongest diffraction at $2\theta = 21°$, which suggests that the long hydrophobic alkyl chains in compound **1** packed with higher order than that in compounds **2** and **3**. The diffraction at $2\theta = 28.5°$, corresponding to a d space of 0.31 or 0.32 nm, can be attributed to the π–π stacking of the trialkyloxylphenyl rings and PDI rings between the adjacent molecules. Two peaks with relative larger intensities appeared in this region in the diffraction pattern of compound **3**, which suggests that the π system in compound **3** stacked with higher order than that in compounds **2** and **1**, and that the π–π interactions are the dominating driving force for the self-assemble process of compound **3**.

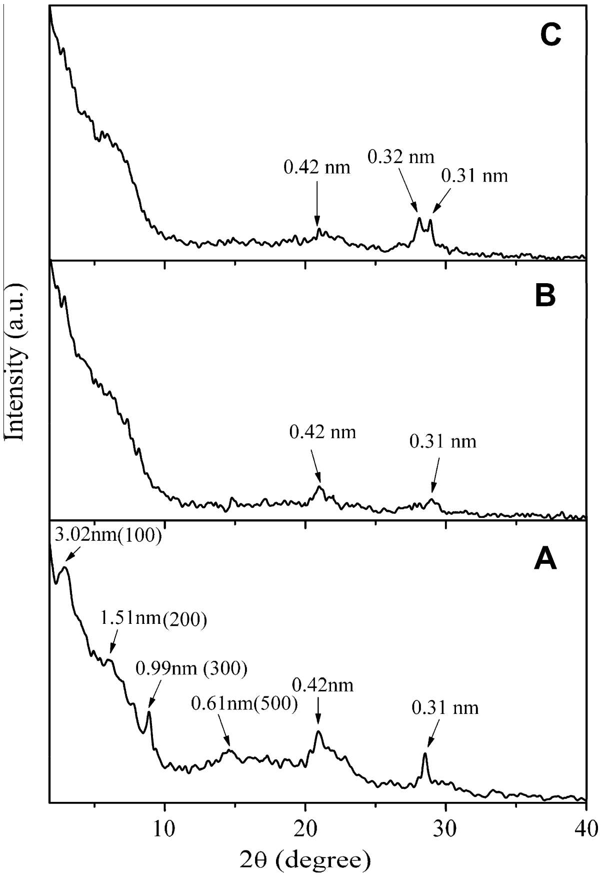

Fig. 5. XRD patterns of the thin solid films of compounds **1**–**3** (A–C) prepared from evaporation of drops of toluene solution on silicon surface.

In the low angle region of the diffraction pattern of compound **1**, a peak at $2\theta = 2.92°$ ($d = 3.02$ nm) can be found, which is accompanied with three higher order refractions at 1.51, 0.99 and 0.61 nm respectively. The diffraction at 3.02 nm is ascribed to the (1 0 0) plane while the peaks at 1.51, 0.99 and 0.61 are ascribed to the (2 0 0), (3 0 0), and (5 0 0) planes accordingly. The minimized molecular structure of compound **1** and the dimensional sized are shown in Fig. 6A. The hydrophobic part (the long alkyl chains, the phenyl rings and the triazine rings) has a semi-circular shape with a radius of about 3.0 nm and a thickness of about 0.8 nm. To achieve the biggest hydrophobic interactions between the neighboring molecules, the semi-circular hydrophobic part must take an ideal "face-to-face" stack as shown in Fig. 6C. Therefore, the preferred direction of the growth of the molecular aggregates driven by the hydrophobic interactions of long alkyl chains is along the axis which perpendicular to the "plane" of the semi-circular hydrophobic part and finally leads to the formation of linear molecular aggregates. Because of the large thickness of the hydrophobic part, the PDI rings of adjacent molecules of compound **1** can not pack closely and therefore, no ground state interactions were observed in the absorption spectra. The d space of the diffraction peak at $2\theta = 2.92°$ is thoroughly equal to the radius of the semi-circular hydrophobic part of the molecule as indicated in Fig. 6, and therefore can be attributed to the thickness of the hydrophobic shell of the linear molecular aggregates.

However, the thin solid films of compounds **2** and **3** do not show any other meaningful diffraction in the low angle region as shown in Fig. 5, which suggests that the molecules in the thin solid films of compounds **2** and **3** pack with less molecular order than that of compound **1**, probably because of the small hydrophobic interactions between the neighboring molecules.

3.7. Morphology of the aggregates

The morphology of the aggregates formed is examined by scanning electron microscopy (SEM). Samples were prepared by drop-casting 1 mg/ml toluene solution of compounds **1**–**3**, respectively, onto the surface of SiO_2 substrate. The SEM images of aggregates of compounds **1**–**3** are shown in Fig. 7. As shown in Fig. 7A, driven mainly by the inter-molecular hydrophobic interactions between side chains, compound **1** self-assemble into one-dimensional (1D) micro-structure with nano-rod morphology. The length of the nano-rod is found to be several micrometers while the width is about 300–500 nm. Based on the results of UV–vis and XRD experiments, we propose that the molecules of compound **1** form linear aggregates first, in which the PDI cores arrange in a "side-by-side" way and the semi-circular hydrophobic part stack in a "face-to-face" mode along the longitudinal direction of the linear aggregates (1-D *J*-aggregates) as shown in Fig. 6E, then several linear aggregates adhere together to form the nano-rod (Fig. 6F) [51]. It is worth noting that the overlap between the semi-circular hydrophobic parts of compound **1** do not induce any changes on the absorption spectra of PDI part due to the large thickness of the hydrophobic part, which hindered the closely packing of the PDI rings in the aggregates (Fig. 6C). The self-assemble process of compound **1** from solution to solid states is schematically summarized in Fig. 6.

On the other hand, both the UV–vis and XRD experiments of compound **3** suggest that its molecules stacked along the perpendicular direction of the aromatic plane driven dominantly by the inter-molecular π–π interaction, leading to the co-facial

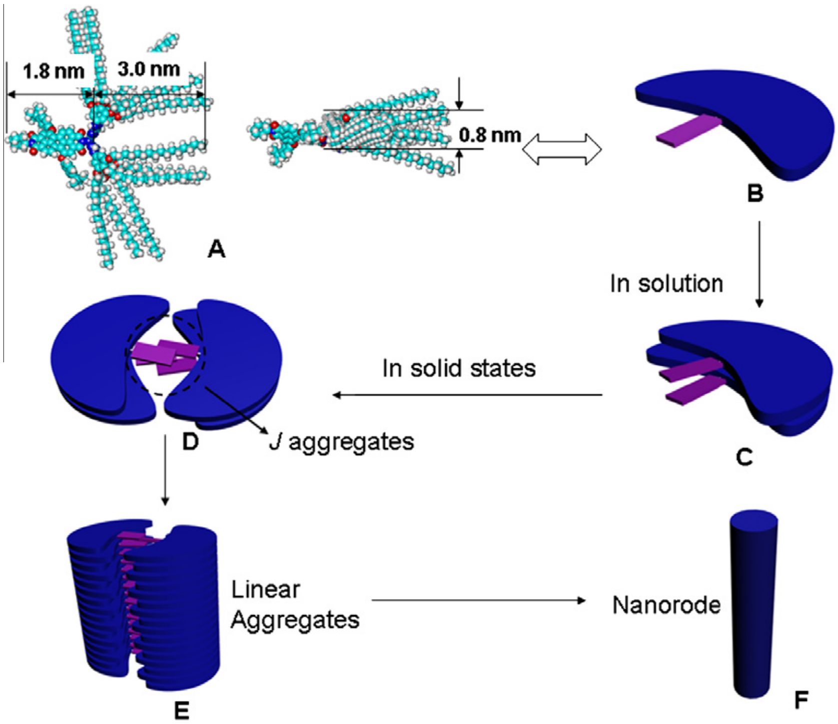

Fig. 6. The minimized structure of compound **1** (A), and its schematic aggregation process in solution (C) and in solid states (D–F).

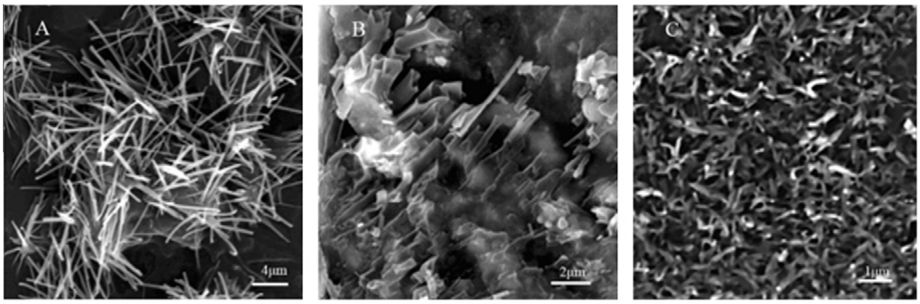

Fig. 7. SEM images of compounds **1**–**3** (A–C) solid film prepared from evaporation of drops of their toluene solution on silicon surface.

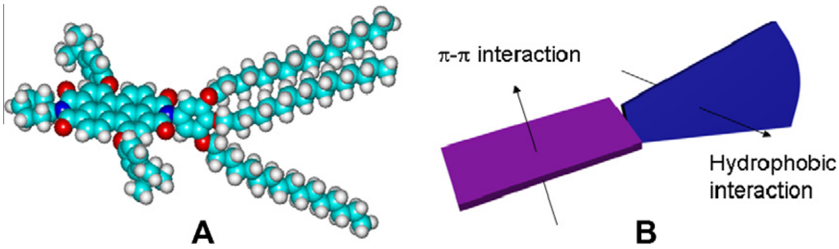

Fig. 8. The minimized molecular structure of compound **3** (A), arrows in the right picture indicates the preferred directions of π–π interaction and hydrophobic interaction.

aggregation and one-dimensional molecular self-assembly. Due to the phenyl ring connected at the imide nitrogen atom preferred a perpendicular conformation relative to the plane of PDI ring as revealed in the minimized structure of compound **3** in Fig. 8, the hydrophobic interactions will drive the molecules aggregate in a different direction from that of π–π stacking and thus induce the formation of ribbon like structure. The ribbon structure appears as a typical assembly produced from the one-dimensional aggregation (1-D *H*-aggregates) as reported in literature [52]. However, compound **2** shows bended sheet-like or tube-like aggregates, implying a molecular packing distorted from both typical co-facial conformation and "side-by-side" arrangement, due to the interference between the π–π interactions and hydrophobic interactions.

4. Conclusion

Three wedge-shaped PDI compounds with a different number of long alkyl chains connected at one end of the molecule are successfully prepared. Because of the strong hydrophobic interactions between the long alkyl chains, these molecules in solution can form aggregates even at extremely low concentrations. For compound **1**, because of the presence of twelve alkyl chains, the hydrophobic interactions between the molecules are extremely strong and dominate the aggregation process. The effects of the π–π interactions between the PDI cores on the aggregation are negligible. With the decrease of the number of the alkyl chains, the hydrophobic interactions between the alkyl chains decrease accordingly and the π–π interactions between the PDI cores begin to affect the aggregation. Compound **3,** with only 3 long alkyl chains, formed *H* aggregates in solution as well as in solid states. Compound **2**, with 6 long alkyl chains, formed *J* aggregates in solution and *H* aggregates in solid states. Because of the interference between the hydrophobic interaction and π–π interaction, the packing order of the molecules of compounds **2** and **3** in solid states decreased significantly. This result demonstrates clearly that the relative strength of different supramolecular interactions could vary the structure of the molecular aggregates and morphology efficiently. It is possible to achieve a fully control of the structure and morphology of the molecular self-assembly by careful designing on molecular structure and programming on different supramolecular interactions. This is very important for the design of new organic self-assemble functional materials for the application in the fields like field-effects transistors and organic solar cells.

Acknowledgment

Financial support from the Natural Science Foundation of China (20771066, 20871055 and 20640420467), Ministry of Education of China and Shandong University, is gratefully acknowledged.

Appendix A. Supplementary data

Supplementary data associated with this article can be found, in the online version, at doi:10.1016/j.jcis.2010.07.012.

References

[1] J. Feng, B. Liang, X. Li, Langmuir 24 (2008) 11209–11215.
[2] B.A. Gregg, J. Phys. Chem. 107 (2003) 4688–4698.
[3] R.A. Cormier, B.A. Gregg, Chem. Mater. 10 (1998) 1309–1319.
[4] C. Kohl, T. Weil, J. Qu, K. Müllen, Chem. Eur. J. 10 (2004) 5297–5310.
[5] J.M. Lehn, Science 295 (2002) 2400–2403.
[6] G.M. Whitesides, J.P. Mathias, C.T. Seto, Science 254 (1991) 1312.
[7] S. Tanaka, M. Shirakawa, K. Kaneko, M. Takeuchi, S. Shinkai, Langmuir 21 (2005) 2163–2172.
[8] X. Li, L.E. Sinks, B. Rybtchinski, M.R. Wasielewski, J. Am. Chem. Soc. 126 (2004) 10810–10811.
[9] L.E. Sinks, B. Rybtchinski, M. Iimura, X. Li, M.R. Wasielewski, Chem. Mater. 17 (2005) 6295–6303.
[10] W. Wang, J.J. Han, L. Wang, L.S. Li, W.J. Shaw, A.D.Q. Li, Nano Lett. 3 (2003) 455–458.
[11] I.K. Iverson, S.M. Casey, W. Seo, S.W. Tam-Chang, Langmuir 18 (2002) 3510–3516.
[12] S. Yagai, T. Seki, T. Karatsu, A. Kitamura, F. Würthner, Angew. Chem. Int. Ed. 47 (2008) 3367–3371.
[13] J.J. Gorp, J.A.J.M. Vekemans, E.W. Meijer, J. Am. Chem. Soc. 124 (2002) 14759–14769.
[14] V. Dehm, Z. Chen, U. Baumeiste, P. Prins, L.D.A. Siebbeles, F. Würthner, Org. Lett. 9 (2007) 1085–1088.
[15] K. Muthukumaran, R.S. Loewe, C. Kirmaier, E. Hindin, J.K. Schwartz, I.V. Sazanovich, J.R. Diers, D.F. Bocian, D. Holten, J.S. Lindsey, J. Phys. Chem. B 107 (2003) 3431–3442.
[16] P. Yan, A. Chowdhury, M.W. Holman, D.M. Adams, J. Phys. Chem. B 109 (2005) 724–730.
[17] M. Andersson, L.E. Sinks, R.T. Hayes, Y. Zhao, M.R. Wasielewski, Angew. Chem. Int. Ed. 42 (2003) 3139–3143.
[18] M.J. Ahrena, M.J. Fuller, M.R. Wasielewski, Chem. Mater. 15 (2003) 2684–2686.
[19] X. Zhang, Z. Chen, F. Würthner, J. Am. Chem. Soc. 129 (2007) 4886–4887.
[20] F.J.M. Hoeben, P. Jonkheijm, E.W. Meijer, A.P.H.J. Schenning, Chem. Rev. 105 (2005) 1491–1546.
[21] Y. Wang, Y. Chen, R. Li, S. Wang, W. Su, P. Ma, M.R. Wasielewski, X. Li, J. Jiang, Langmuir 23 (2007) 5836–5842.
[22] Z. Chen, V. Stepanenko, V. Dehm, P. Prins, L.D.A. Siebbeles, J. Seibt, P. Marquetand, V. Engel, F. Würthner, Chem. Eur. J. 13 (2007) 436–449.
[23] F. Würthner, C. Thalacker, S. Diele, C. Tschierske, Chem. Eur. J. 7 (2001) 2245–2253.
[24] M.J. Fuller, L.E. Sinks, B. Rybtchinski, J.M. Giaimo, X. Li, M.R. Wasielewski, J. Phys. Chem. A 109 (2005) 970–975.
[25] Y. Che, X. Yang, S. Loser, L. Zang, Nano Lett. 8 (2008) 2219–2223.
[26] V. Percec, C.H. Ahn, T.K. Bera, G. Ungar, D.J.P. Yeardley, Chem. Eur. J. 5 (1999) 1070–1083.
[27] C. Devadoss, P. Bharathi, J.S. Moore, J. Am. Chem. Soc. 118 (1996) 9635–9644.
[28] W. Wang, L.S. Li, G. Helms, H.H. Zhou, A.D.Q. Li, J. Am. Chem. Soc. 125 (2003) 1120–1121.
[29] K. Balakrishnan, A. Datar, R. Oitker, H. Chen, J. Zuo, L. Zang, J. Am. Chem. Soc. 127 (2005) 10496–10497.
[30] M.J. Ahrens, L.E. Sinks, B. Rybtchinski, W. Liu, B.A. Jones, J.M. Giaimo, A.V. Gusev, A.J. Goshe, D.M. Tiede, M.R. Wasielewski, J. Am. Chem. Soc. 126 (2004) 8284–8294.
[31] Y. Che, A. Datar, K. Balakrishnan, L. Zang, J. Am. Chem. Soc. 129 (2007) 7234–7235.
[32] A.E. Clark, C. Qin, A.D.Q. Li, J. Am. Chem. Soc. 129 (2007) 7586–7595.
[33] J. Feng, Y. Zhang, C. Zhao, R. Li, W. Xu, X. Li, J. Jiang, Chem. Eur. J. 14 (2008) 7000–7010.
[34] G. Lu, Y. Chen, Y. Zhang, M. Bao, Y. Bian, X. Li, J. Jiang, J. Am. Chem. Soc. 130 (2008) 11623–11630.
[35] S. Ghosh, X.-Q. Li, V. Stepanenko, F. Würthner, Chem. Eur. J. 14 (2008) 11343–11357.
[36] Y. Chen, Y. Kong, Y. Wang, P. Ma, M. Bao, X. Li, J. Colloid Int. Sci. 330 (2009) 421–427.
[37] Wei Su, Y. Zhang, Ch. Zhao, X. Li, J. Jiang, Chem. Phys. Chem. 8 (2007) 1857–1862.
[38] M. Vacha, M. Furuki, L.S. Pu, K. Hashizume, T. Tani, J. Phys. Chem. B 105 (2001) 12226–12229.
[39] F. Würthner, Z. Chen, V. Dehm, V. Stepanenko, Chem. Commun. (2006) 1188.
[40] X. Yang, X. Xu, H. Ji, J. Phys. Chem. B 112 (2008) 7196–7202.
[41] K. Balakrishnan, A. Datar, T. Naddo, J. Huang, R. Oitker, M. Yen, J. Zhao, L. Zang, J. Am. Chem. Soc. 128 (2006) 7390–7398.
[42] G. Klebe, F. Graser, E. Hadicke, J. Berndt, Acta Crystallogr. B45 (1989) 69–77.
[43] P.M. Kazmaier, R. Hoffmann, J. Am. Chem. Soc. 116 (1994) 9684–9691.
[44] M.D. Porter, T.B. Bright, D.L. Allara, C.E.D. Chidsey, J. Am. Chem. Soc. 109 (1987) 3559–3568.
[45] R.M. Crooks, C. Xu, L. Sun, S.L. Hill, A. Ricco, J. Spectrosc. 8 (1993) 29–39.
[46] J.P. Hill, W. Jin, A. Kosaka, T. Aida, Science 304 (2004) 1481–1483.
[47] H. Tachibana, N. Hosaka, Y. Tokura, Macromolecules 34 (2001) 1823–1827.
[48] N. Jeon, K. Finnie, K. Branshaw, R.G. Nuzzo, Langmuir 13 (1997) 3382–3391.
[49] S. Singh, J. Wegmann, K. Albert, K. Müller, J. Phys. Chem. B 106 (2002) 878–888.
[50] C.V. Yelamaggad, A.S. Achalkumar, R.D.S. Shankar, S.K. Prasad, J. Org. Chem. 72 (2007) 8308–8318.
[51] X.-Q. Li, V. Stepanenko, Z. Chen, P. Prins, L.D.A. Siebbelesb, F. Würthner, Chem. Commun. (2006) 3871–3873.
[52] L. Zang, Y. Che, J.S. Moore, Acc. Chem. Res. 41 (2008) 1596–1608.